Stress-Sensors with High-Sensitivity Using the Combined Meandering-Patterns

Chun-Hyung Cho[1] and Ho-Young Cha[2]

Abstract—**In this work, the combined meandering-pattern stress-sensors were presented in order to achieve the high sensitivity of stress sensors. Compared to the previous works, which have been using the single meandering-pattern stress-sensors, the sensitivity was approximately observed to increase by 30%~70%. Also, in this paper, more simple and convenient stress-measurement method was presented.**

Index Terms—**Meandering –pattern, sensitivity, stress sensors, piezo-resistive coefficients**

I. INTRODUCTION

Piezo-resistive stress sensors, which have widespread applications as sensing elements in various transducers [1-11], are powerful tools for the experimental structural analysis of electronic packages. Such sensors are to be used to measure stress. Piezo-resistive stress sensor test chips have been successfully used to characterize die stress induced at various steps in the electronic packaging process. Expressions of resistance changes for piezo-resistive stress sensors were derived for stress measurements [6]. In order to utilize these test chips to measure stresses, one must have values of the piezo-resistive (pi) coefficients because the piezo-resistive behavior of such sensors is characterized by three pi-coefficients (π_{11}, π_{12}, and π_{44} for the stress sensors on (001) silicon surface, and B_1, B_2, and B_3 for the stress sensors on (111) silicon surface), which are electro mechanical material constants. The calibration of the piezo-resistive coefficients is normally performed using resistor stress sensors which are conveniently fabricated into the surface of the die using current microelectronic technology.

So far, the traditional single meandering patterns have been used. Sometimes, the optimized sensor rosettes were used for obtaining 3 normal stress components and 3 shear stress components. But this method cannot also enhance the sensitivity of the stress sensor. In this work, we presented the new method to achieve the high sensitivity by combining the individual sensor.

II. REVIEW OF BASIC EQUATIONS

The (111) silicon wafer is most commonly used in the current microelectronics industry. The geometry for the (111) silicon wafers is shown in Fig. 1. The principal crystallographic axes are aligned parallel and perpendicular to the standard wafer flat. A wafer plot showing the direction x'_1 that strips is cut from the (111) wafer in this work is shown in Fig. 1. Note that φ is defined as the angle between the primary axis and the resistor orientation for the coordinate system. The general expression for resistance change under stress is given by [6]

Manuscript received Aug. 13, 2014; accepted Sep. 23, 2014
A part of this work was presented in Asia-Pacific Workshop on Fundamental and Applications of Advanced Semiconductor Devices, Kanazawa, Japan, July. 2014
[1] Department of Electronic & Electrical Engineering, College of Science and Technology, Hongik University, Jochiwon, Sejong, 339-701, Korea
[2] School of Electronic & Electrical Engineering, College of Engineering, Hongik Unversity, 72-1, Sangsu-dong, Seoul, 121-791, Korea
E-mail : chcho@hongik.ac.kr

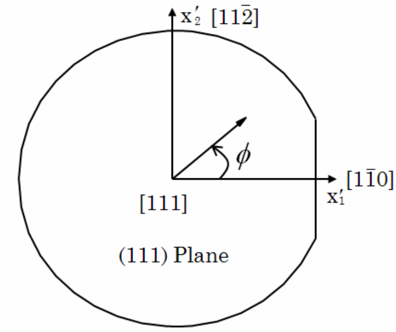

Fig. 1. The (111) silicon wafer geometry.

$$\frac{\Delta R_{\varphi}}{R_{\varphi}} = [B_1\sigma'_{11} + B_2\sigma'_{22} + B_3\sigma'_{33} - 2\sqrt{2}\,(B_2 - B_3)\sigma'_{23}]\cos^2\varphi$$
$$+ [B_2\sigma'_{11} + B_1\sigma'_{22} + B_3\sigma'_{33} + 2\sqrt{2}(B_2 - B_3)\sigma'_{23}]\sin^2\varphi$$
$$+ [2\sqrt{2}(B_3 - B_2)\sigma'_{13} + (B_1 - B_2)\sigma'_{12}]\sin 2\varphi \quad (1)$$

where

$$B_1 = \frac{\pi_{11} + \pi_{12} + \pi_{44}}{2},\ B_2 = \frac{\pi_{11} + 5\pi_{12} - \pi_{44}}{6},$$
$$B_3 = \frac{\pi_{11} + 2\pi_{12} - \pi_{44}}{3}$$

For ϕ = 0 and 90°, considering only uniaxial stress σ'_{11} in previous equations in four-point bending method, Eq. (1) gives

$$\frac{\Delta R_0}{R_0} = B_1\sigma'_{11},\quad \frac{\Delta R_{90}}{R_{90}} = B_2\sigma'_{11} \quad (2)$$

Similarly, the geometry for the (001) silicon wafers of interest here is given in Fig. 2 relative to the primed coordinate system.

For the primed axes, the expression for a resistor sensor at angle ϕ with respect to the x'_1 axis is given by [6]

$$\frac{\Delta R_{\varphi}}{R_{\varphi}} = \left[\left(\frac{\pi_{11} + \pi_{12} + \pi_{44}}{2}\right)\sigma'_{11} + \left(\frac{\pi_{11} + \pi_{12} - \pi_{44}}{2}\right)\sigma'_{22}\right]\cos^2\varphi$$
$$+ \left[\left(\frac{\pi_{11} + \pi_{12} - \pi_{44}}{2}\right)\sigma'_{11} + \left(\frac{\pi_{11} + \pi_{12} + \pi_{44}}{2}\right)\sigma'_{22}\right]\sin^2\varphi$$
$$+ \pi_{12}\sigma_{33} + (\pi_{11} - \pi_{12})\sigma'_{12}\sin 2\varphi \quad (3)$$

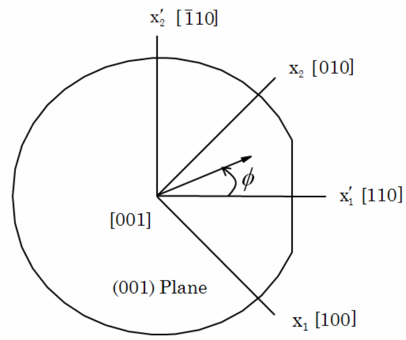

Fig. 2. General (001) silicon wafer geometry.

For ϕ = 0 and 90°, considering only uniaxial stress σ'_{11} in previous equations , Eq. (3) gives

$$\frac{\Delta R_0}{R_0} = \left(\frac{\pi_{11} + \pi_{12} + \pi_{44}}{2}\right)\sigma'_{11},$$
$$\frac{\Delta R_{90}}{R_{90}} = \left(\frac{\pi_{11} + \pi_{12} - \pi_{44}}{2}\right)\sigma'_{11} \quad (4)$$

Note that the temperature is assumed to be maintained constant at the reference temperature and the literature values for pi-coefficients for lightly p-typed doped silicon by [11] are $\pi_{11} = 66$ TPa^{-1}, $\pi_{12} = -11$ TPa^{-1}, and π_{44} = 1381 TPa^{-1}.Therefore, B_1=718 TPa^{-1}, B_2=-228 TPa^{-1}, and B_3=-448 TPa^{-1}.

III. Chip Design and Analysis

We have designed and fabricated a special test chip on the (111) silicon surface. The test chip contains p-type and n-type sensor sets, each with resistor elements making angles of ϕ =0, +45, -45, and 90 with respect to the x'_1 axis. Resistors are often designed with relatively large meandering patterns to achieve acceptable resistance levels for measurement. Our sensors have a peak impurity concentration of 3.0×10^{18}/cm^3 for p-type and 5.0×10^{19}/cm^3 for n-type resistor sensors, respectively. The pattern of our test chip is repeated in the layout throughout the wafer.

Hence, the piezo-resistive coefficients are determined from the slopes of the graphs of resistance versus uniaxial stress. The typical results for the normalized resistance change of R_0 as a function of an applied stress for p-type resistor sensor are shown in Fig. 4. For the primed coordinate system, B_1 corresponds to the slope of

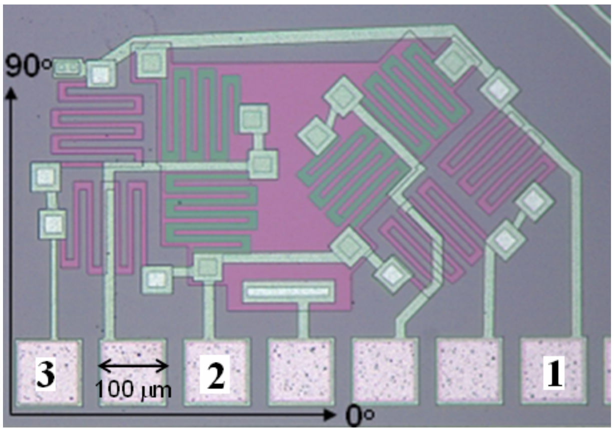

Fig. 3. Microphotograph of an optimized eight-element sensor rosette incorporating four n-type (green) and four p-type (pink) resistor sensors in a (111) silicon test chip (JSE-WB100C). Pads are 100 × 100 μm^2 with 125 μm pitch.

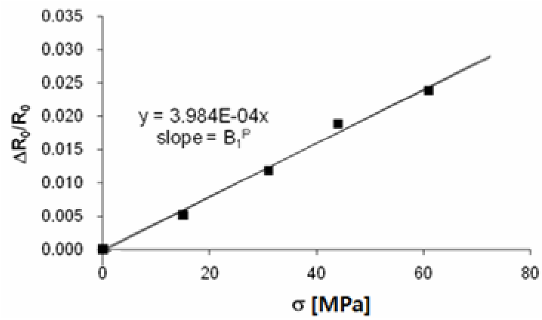

Fig. 4. Typical stress sensitivity of p-type resistor sensors with respect to the primed coordinate system.

$\Delta R_0/R_0$ versus σ'_{11}. The unstressed values of resistance are 10.5 kΩ and 2.27 kΩ for p- and n- type silicon, respectively.

Our measured value of pi-coefficients for the JSE-WB100C die is lower than expected for lightly doped sensors based upon the data of Smith [11]. It is observed that B_1 = 366 TPa^{-1}, B_2 = -134 TPa^{-1} for p-type resistor sensors while, for n-type resistor sensors, B_1 = -133 TPa^{-1}, B_2 = 97.4 TPa^{-1}.

In order to generate the uniaxial stress in the silicon-strip samples, we used the Four-point bending (4 PB). The four-point bending (4 PB) loading fixture is presented in Fig. 5. A force generated by a vertical translation stage is applied to the four-point bending fixture in which the applied stress is independent of the location and is uniform as long as the sensor is located between the inner supports. The applied force is calculated from the output of the load-cell. The uniaxial stress σ'_{11} at points on the top surface of the strip is given

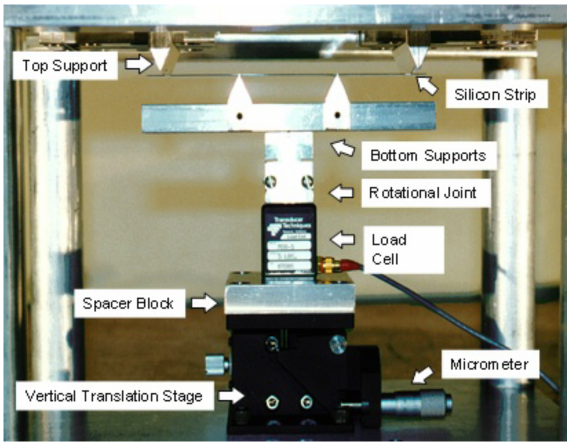

Fig. 5. Four-point bending loading fixture.

by σ'_{11} =3 F(L-D)/(ht^2), where h is the beam width, t is the beam thickness, L is the distance between the two top supports, and D is the distance between the two bottom supports.

As presented in Fig. 3, the 0°/90° resistor sensors are connected. We applied the constant voltage between pad-2 (1 V) and pad-1 (GND). For an n-substrate, the voltage is set to be 2 V for electrical isolation between the doped surface resistor and substrate regions by using proper reverse biasing. Note that pad-3 is the mid-point of the pair. During the application of stress σ'_{11}, we analyzed R_0/R_{90} in terms of σ'_{11}. In the process, we define A as the slope of R_0/R_{90} with respect to σ'_{11}. R_0/R_{90} can be expressed as

$$\frac{R_0(\sigma'_{11})}{R_{90}(\sigma'_{11})} = A\sigma'_{11} + \frac{R_0(0)}{R_{90}(0)} \tag{5}$$

where $R(\sigma'_{11})$ is the stressed-resistance while R(0) is the unstressed-resistance.

$$\frac{R_0(0)}{R_{90}(0)}\left[\frac{1+B_1\sigma'_{11}}{1+B_2\sigma'_{11}}\right] = A\sigma'_{11} + \frac{R_0(0)}{R_{90}(0)} \tag{6}$$

Then we let $\frac{R_0(0)}{R_{90}(0)} \equiv C$ with the following result:

$$C\left[\frac{1+B_1\sigma'_{11}}{1+B_2\sigma'_{11}}\right] = A\sigma'_{11} + C \tag{7}$$

Note that B_1 and B_2 for silicon have the unit of hundreds/TPa (= 10^{-10} order). Also, stress σ'_{11} is restricted to less than 100 MPa due to the stiff characteristic of silicon. Generally it has dozens MPa(= 10^7 order). Hence, $B_1\sigma'_{11}$ and/or $B_2\sigma'_{11}$ have the order of 10^{-3}~10^{-2}. Using $B_1\sigma'_{11} << 1$ and $B_2\sigma'_{11} << 1$, the result becomes:

$$C(1+B_1\sigma'_{11}-B_2\sigma'_{11}) = A\sigma'_{11}+C$$
$$(B_1-B_2)\sigma'_{11} = \frac{A}{C}\sigma'_{11} \quad (8)$$

where $C \cong 1$ for both p- and n-type because the fabricated 0°/90° resistor sensors are from the same batch. It yields

$$(B_1-B_2) = A \quad (9)$$

By performing multiple measurements, we determined the validity of Eq. (9) as seen in Table 1. The calibration results are in good with Eq. (9). If we measure R_{90}/R_0 instead of R_0/R_{90}, the slope of R_{90}/R_0 with respect to σ'_{11} will be (B_2-B_1). Note that the sensitivity will be unchanged but the sign will be opposite.

In the previous works, a single meandering-pattern stress-sensor was used. However, for higher sensitivity, the combined meandering-pattern stress-sensors were newly used in this study. Considering only uniaxial stress σ'_{11} in Eq. (1) gives the maximum and/or minimum rate of $\Delta R/R$ with respect to σ'_{11} occurs at ϕ =0 and/or ϕ =90 as presented in Eq. (10).

$$\frac{\partial}{\partial\varphi}\left(\frac{\Delta R_\varphi}{R_\varphi}\right) = \frac{\partial}{\partial\varphi}\left([B_1\sigma'_{11}]\cos^2\varphi+[B_2\sigma'_{11}]\sin^2\varphi\right)$$
$$= -2\cos\varphi\sin\varphi(B_1-B_2)\sigma'_{11}$$
$$= -\sin 2\varphi(B_1-B_2)\sigma'_{11} = 0 \quad (10)$$

where the highest sensitivity occurs at ϕ =0.

$$\frac{\partial}{\partial\varphi}\left(\frac{[\frac{\Delta R_\varphi}{R_\varphi}]}{[\frac{\Delta R_{\varphi+90}}{R_{\varphi+90}}]}\right) = \frac{\partial}{\partial\varphi}\left(\frac{[B_1\cos^2\varphi+B_2\sin^2\varphi]}{[B_2\cos^2\varphi+B_1\sin^2\varphi]}\right)$$
$$= \frac{\sin 2\varphi(B_2-B_1)(B_2\cos^2\varphi+B_1\sin^2\varphi)-(B_1\cos^2\varphi+B_2\sin^2\varphi)\sin 2\varphi(B_1-B_2)}{(B_2\cos^2\varphi+B_1\sin^2\varphi)^2}$$
$$= \frac{\sin 2\varphi(B_2-B_1)(B_1+B_2)}{(B_2\cos^2\varphi+B_1\sin^2\varphi)^2} = 0$$

Table 1. Comparison between (B_1-B_2) and A (= slope of R_0/R_{90} versus σ'_{11}) by measurements at room temperature

	p-type[TPa^{-1}]	n-type[TPa^{-1}]
(B_1-B_2)	500	-231
A	476	-226
Error (%)	-4.8%	-2.1%

Table 2. Comparison of sensitivity between the conventional “Single” and the proposed “Combined”

	p-type[TPa^{-1}]	n-type[TPa^{-1}]
Single	366	-133
Combined	476	-226
Increase (%)	30.1%	69.9%

the maximum and/or minimum rate of $(\Delta R_\phi/R_\phi)/(\Delta R_{\phi+90}/R_{\phi+90})$ with respect to σ'_{11} occurs at ϕ =0 and/or ϕ =90.

Table 2 compares the highest sensitivity for ϕ =0 between a single meandering-pattern and the combined meandering-pattern. By using the combined pair, the sensitivity was approximately increased by 30.1% and 69.9% for p- and n-type resistor sensors, respectively.

Conventionally, for the measurement of the sensitivity, current must be measured for the voltage applied across the sensor. In order to see the change in resistance with respect to the applied stresses, the measurement of current is needed for each and every single measurement. However, this work does not need to measure current. Only the measurement of the change in voltage of the mid-point (pad-3) versus the applied stress is required. Therefore, this work presents the more convenient calibration of the sensitivity.

IV. Summary

Conventionally, in order to measure the sensitivity, a single meandering-pattern stress-sensor was used. However, in this work, we have designed the combined meandering-pattern stress-sensors on (111) silicon surface. Then, we analyzed the sensitivity of the combined ones. Compared to the previous works, the sensitivity was observed to increase significantly. For p- and n-type resistor sensors, the sensitivity was increased by 30.1% and 69.9%, respectively.

Also, this work proposed the simple and convenient stress-measurement method in which the measurement of current is not required, however, the measurement of voltage of the mid-point is needed. Note that doping concentration affects the sensitivity of the stress sensor. As doping concentration increases, the sensitivity decreases. However, the proposed method will dramatically enhance the sensitivity at any doping level.

V. FUTURE WORKS

In the future, the new fabrication method for the elimination of transverse-effect, which decreases the sensitivity, will be investigated. In addition, two pairs of $0^o/90^o$ resistor-sensors, instead of one pair, will be used for much higher sensitivity.

ACKNOWLEDGMENTS

The authors gratefully acknowledge the support of the Alabama Microelectronics Science and Technology Center (AMSTC) and the NSF Center for Advanced Vehicle Electronics (CAVE). This work (Grants No. C0213722) was supported by Business for Cooperative R&D between Industry, Academy, and Research Institute funded Korea Small and Medium Business Administration in 2014. Also, this work was supported by 2014 Hongik University Research Fund.

REFERENCES

[1] Kanda, Y., "Graphical Representation of the Piezoresistance Coefficients in Silicon," *IEEE Transactions on Electron Devices*, vol. 29(1), pp. 64-70, 1982.

[2] Bittle, D. A., Suhling, J. C., Beaty, R. E., Jaeger, R. C., and Johnson, R. W., "Piezoresistive Stress Sensors for Structural Analysis of Electronic Packages," *Journal of Electronic Packaging*, vol. 113(3), pp. 203-215, 1991.

[3] Matsuda, Kazunori., "Nonlinear Piezoresistance Effects in Silicon," *J. Appl. Phys*.,vol.73(4), pp. 1838-1847, 1993.

[4] Jaeger, R. C., Suhling, J. C., Ramani, R., "Errors Associated with the Design, Calibration of Piezoresistive Stress Sensors in (100) Silicon," *IEEE Transactions on Components, Packaging, and Manufacturing Technology - Part B: Advanced Packaging*, vol. 17(1), pp. 97-107, 1994.

[5] Lund, Einvind., Finstad, T., "Measurement of the Temperature Dependency of the Piezoresistance Coefficients in p-type Silicon," *EEP-vol.26-1, Advances in Electronic Packaging*, vol. 1 ASME 1999, pp. 215-218, 1999.

[6] J. C. Suhling and R. C. Jaeger, "Silicon piezoresistive stress sensors and their application in electronic packaging", *IEEE Sensors Journal*, vol. 1, no. 1, pp. 14-30, June 2001.

[7] J. Richter and O. Hansen, "Piezoresistance of silicon and strained $Si_{0.9}Ge_{0.1}$", *Sensors and Actuators A* 123-124, pp. 388-396, 2005.

[8] Mian, A., Suhling, J. C., and Jaeger, R. C., The van der Pauw stress sensors, *IEEE Sensors Journal*, vol. 6, no. 2, pp. 340-356, April, 2006.

[9] Cho, C.-H., Jaeger, R. C., Suhling, J. C., "Evaluation of the Temperature Dependence of the Combined Piezoresistive Coefficients of (111) Silicon Utilizing Chip-on-Beam and Hydrostatic Calibration," *JKPS*, vol. 52, No. 3, pp. 612-620, 2008.

[10] Cho, C.-H., Jaeger, R. C., Suhling, J. C., "Characterization of the Temperature Dependence of the Piezoresistive Coefficients of Silicon from -150°C to +125°C," *IEEE Sensors Journal*, vol.8, No. 8, pp. 1455-1468, 2008.

[11] C. S. Smith, "Piezoresistance effects in germanium and silicon", *Physical Review*, vol. 94 (1), pp. 42-49, December, 1954.

Chun-Hyung Cho received the B.S. degree in Electrical Engineering from the Seoul National University, Seoul, South Korea, in 1997, and the M.S. and ph.D. degrees in Electrical and Computer Engineering from Auburn University, Auburn, AL, in 2001 and 2007, respectively. In 2009, he joined Hongik University, Sejong where he is currently an assistant professor in the Department of Electronic & Electrical engineering. His research interests include the application of analytical and experimental methods of piezoresistive sensors to problems in electronic packaging.

Ho-Young Cha received the B.S. and M.S. degrees in electrical engineering from from Seoul National University, Seoul, Korea, in 1996 and 1999, respectively, and the Ph.D. degree in electrical and computer engineering from Cornell University, Ithaca, NY, in 2004. He was a Postdoctoral Research Associate with Cornell University until 2005, where he focused on the design and fabrication of SiC and GaN electronic devices and GaN nanowires. He was with the General Electric Global Research Center, Niskayuna, NY, from 2005 to 2007, developing wide-bandgap semiconductor sensors and high power devices. Since 2007, he has been with Hongik University, Seoul, where he is currently an Associated Professor in the School of Electronic and Electrical Engineering. His research interests include wide bandgap semiconductor devices. He has authored over 60 publications in his research area.